6ICEGE 6th International Conference on Earthquake Geotechnical Engineering
1-4 November 2015
Christchurch, New Zealand

Overturning of Buildings Induced by Tsunami Run-up At Onagawa in the 2011 Great Tohoku Earthquake

M. Ishida[1], K. Tokimatsu[2], S. Inoue[3]

ABSTRACT

The tsunami caused by the 2011 Great Tohoku Earthquake inflicted substantial damage on structures along the east Japanese coast. The town of Onagawa was one of the most heavily damaged areas, and had an inundation height up to 14.8 m. The most remarkable feature in this area is that reinforced concrete buildings overturned and the type of building damage varied considerably. For example, one pile foundation building overturned landward and one spread foundation building overturned seaward. To investigate the differences in damage type, we conducted a two dimensional tsunami run-up simulation using video evidence as input data. Based on the time histories of inundation height and flow velocity predicted by this simulation, we estimated the hydrodynamic force and buoyant force acting on three buildings. The results of the analysis were able to qualitatively predict the differences in damage mechanism and overturning direction.

Introduction

The huge tsunami caused by the 2011 Great Tohoku Earthquake (Mw 9.0), which occurred at 14:46 on 11 March 2011, inflicted substantial damage on numerous structures along the east coast of Japan. The town of Onagawa, located on the coast in Miyagi Prefecture, was one of the most heavily damaged areas, with an inundation height at Onagawa port of up to 14.8m. The most remarkable feature in this area is that reinforced concrete (RC) buildings overturned and the type of building damage varied considerably. For example, one pile foundation building overturned landward and one spread foundation building overturned seaward. Sugimura et al. (2012) indicated several factors that may have caused overturning, such as hydrodynamic force, buoyant uplift force, scour and liquefaction of the underlying soil, and debris impact. However, it is not clear which factor or combination of factors is the main cause of overturning. Therefore, it is necessary to evaluate the cause of overturning to prevent similar damage from future tsunamis.

To investigate the influence of different factors on tsunami damage, this study conducted a two dimensional (2D) simulation of the 2011 Great Tohoku Earthquake tsunami in Onagawa using video evidence of the first tsunami run-up (Koshimura et al., 2012). Based on the time histories of inundation height and flow velocity predicted by the 2D simulation, we estimate the hydrodynamic forces and buoyant forces acting on three buildings and attempt to qualitatively predict the building damage with overturning direction.

[1]ISHIDA Michitaka, Graduate Student, Tokyo Institute of Technology, Japan, ishida.m.ab@m.titech.ac.jp
[2]TOKIMATSU Kohji, Professor, Tokyo Institute of Technology, Japan, tokimatsu@arch.titech..ac.jp
[3]INOUE Shusaku, Associate Chief Researcher, Takenaka Corporation, Japan, inoue.shuusaku@takenaka.co.jp

Description of buildings examined

Figure 1 shows the location and overturning direction of the three buildings examined in this study. Buildings No.1 overturned landward, building No.3 overturned seaward, and building No.2 did not overturn and remained at its original position. Figure 2a is a photograph of the first tsunami run-up at its maximum inundation height, and Figure 2b is a photograph taken during the tsunami backwash. Based on the photographs, we conclude that the overturning damage occurred during the first tsunami run-up.

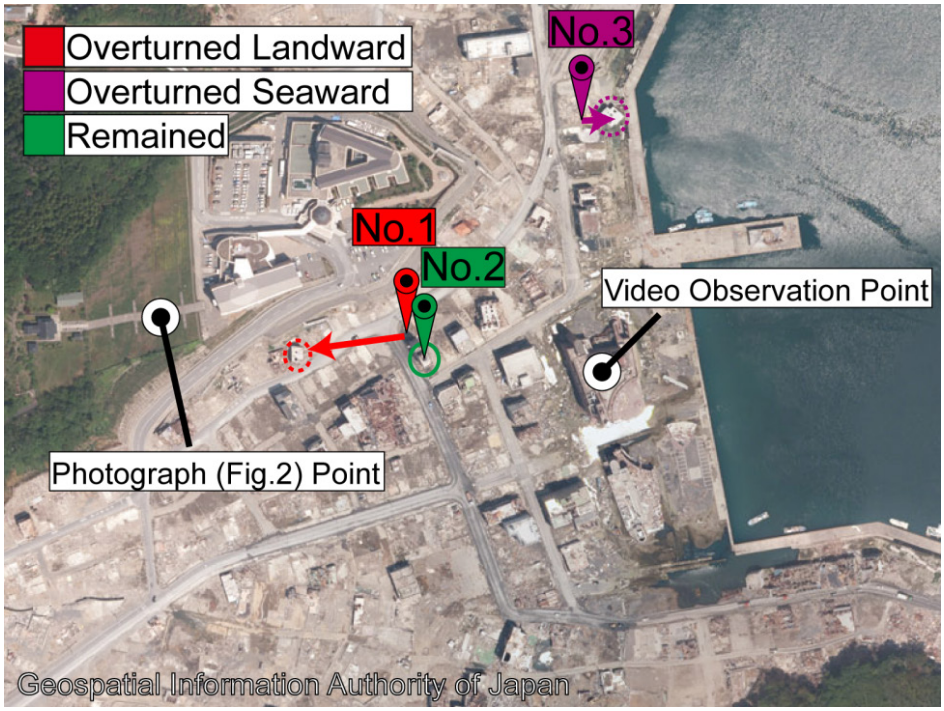

Figure 1. The point and overturning direction of buildings

(a) At maximum inundation height

(b) At backwash

Figure 2. 1st tsunami run-up

Figure 3 shows building No.1, a four-story RC building with pile foundation that overturned landward and displaced 70m from its original position. The pile foundation had 32 RC piles 4m long and 300mm in diameter, and all piles except one were broken at or near the pile head. One pile was pulled 3m up at its original position, and the exposed steel reinforcement had cut and thinning ends. This type of break is caused by tensile failure, which means that the piles were able to generate pull-out resistance.

(a)After the tsunami (b) Pile of No.1 at its original position

Figure 3. Damage overview of building No.1

Figure 4 shows building No.2, a five-story RC building with pile foundation that was situated next to Building No.1 but did not overturn or displace. At this site, the ground subsidence indicates soil liquefaction (Tokimatsu et al., 2012). However, because the piles of Building No.1 were able to generate pull-out resistance, we assume in the following discussion that the effects of soil liquefaction on reducing the pull-out resistance of Building No.2 are negligible.

Figure 5 shows building No.3, a four-story RC building with spread foundation that toppled and displaced 10m from its original position. This is the only building that overturned seaward. The fourth floor of the building detached and is missing

(a) Before the tsunami (b) After the tsunami

Figure 4. Damage overview of building No.2

(a) Before the tsunami (b) After the tsunami

Figure 5. Damage overview of building No.3

Modeling of buildings

Figure 6 shows the elevations with openings of each building on three sides. The building elevations were determined based on outfield surveys and photographs taken before the earthquake. Figure 6 shows that all buildings except building No.2 were completely submerged at the maximum inundation height.

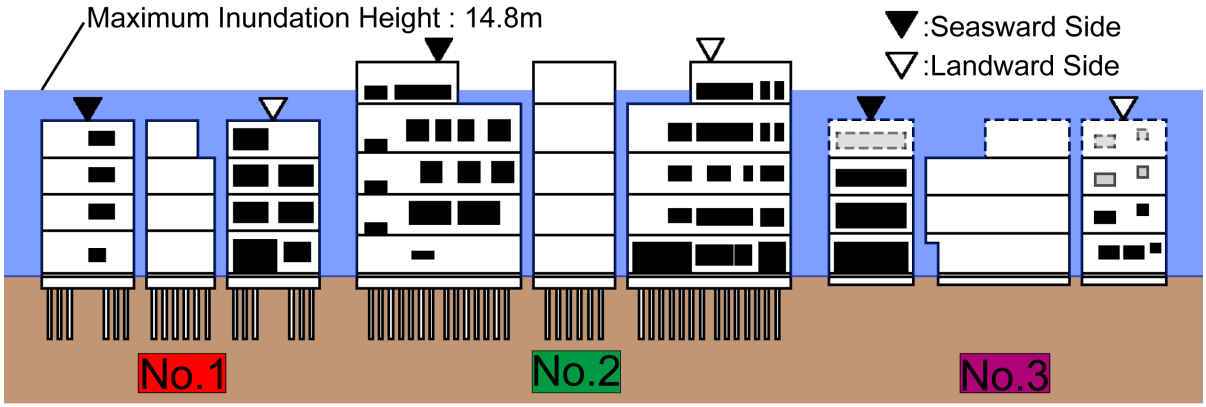

Figure 6. Elevations of buildings

We estimated the building weight by assuming the weight per unit area of the RC buildings and foundations was 13kN/m^2.

Based on the pile profiles, we assumed that the RC piles of building No.1 were spun concrete piles according to JIS A 5310 standard. We estimated the compressive strength of the concrete as 40N/mm^2 and the tensile strength of the rebar as 400N/mm^2 in the RC piles. The piles of building No.2 were assumed to be the same as building No.1.

The pile pull-out resistance force R_{tc} was estimated as;

$$R_{tc} = Wp + \varphi \times \Sigma \tau_{st} \times L_s \quad (1)$$

where W_p is the pile weight, φ is the pile circumference, L_s is the pile length, and τ_{st} is the friction stress of the pile in the sand layers calculated as 2N, where N is the Swedish Ram Sounding values obtained by Kiku et al. (2012) at the locations of each of the two pile foundation buildings after the earthquake.

Evaluation of tsunami load

A 2D simulation of tsunami run-up is performed with a shallow water theory (Hirt and Richardson, 1999). Figure 7 shows the calculation area. The lengths of X direction and Y direction are 1530m and 570m, and the mesh size is 10m by 10m. In Figure 8, the broken and solid black lines are the estimated inundation height and flow velocity from video analysis (Koshimura et al., 2012), respectively. The red line is the smoothed inundation height that was used as the input boundary condition to simulate the tsunami wave. Figure 8 also shows the calculated inundation height (green line) and flow velocity in the X direction (blue line) at the point where the video was taken. The inundation height and flow velocity calculated by the simulation correspond well to the values estimated from the video analysis, except at 15:26 when the simulation predicts slightly slower flow velocity than the video analysis. Figure 9 shows the distribution of the inundation height and flow velocity calculated by the simulation. The inundation area shown in Fig.9 by the simulation corresponds well to the actual condition.

The hydrodynamic force F_D acting on the buildings is calculated by the following formula (FEMA P646, 2008);

$$F_D = 1/2 \times \rho \times C_D \times u^2 \times h \times B \quad (2)$$

where ρ is the fluid density including sediment ($1.2t/m^3$), C_D is the drag coefficient (2.0), u and h are the flow velocity and inundation height calculated by the 2D simulation analysis, and B is the building width.

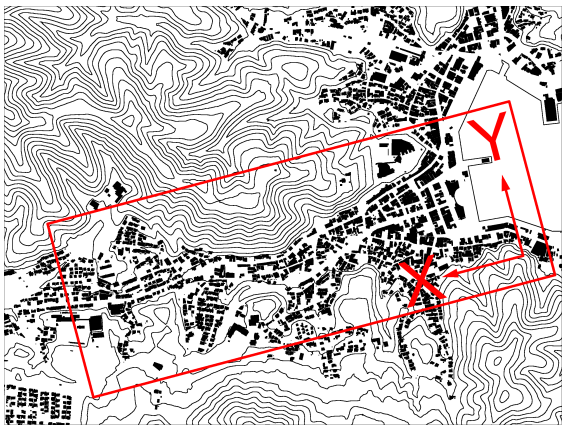

Figure 7. Calculation area

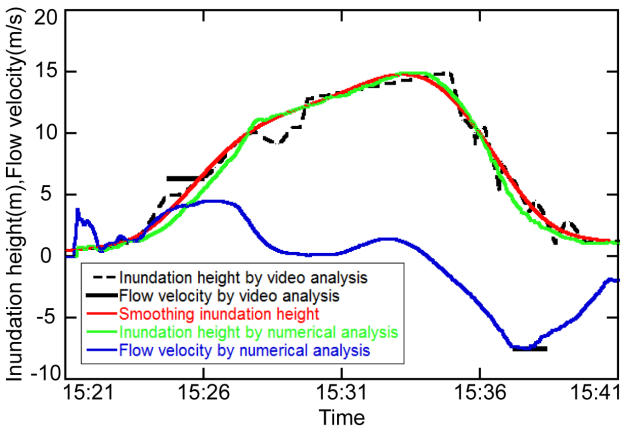

Figure 8. Inundation height and flow velocity

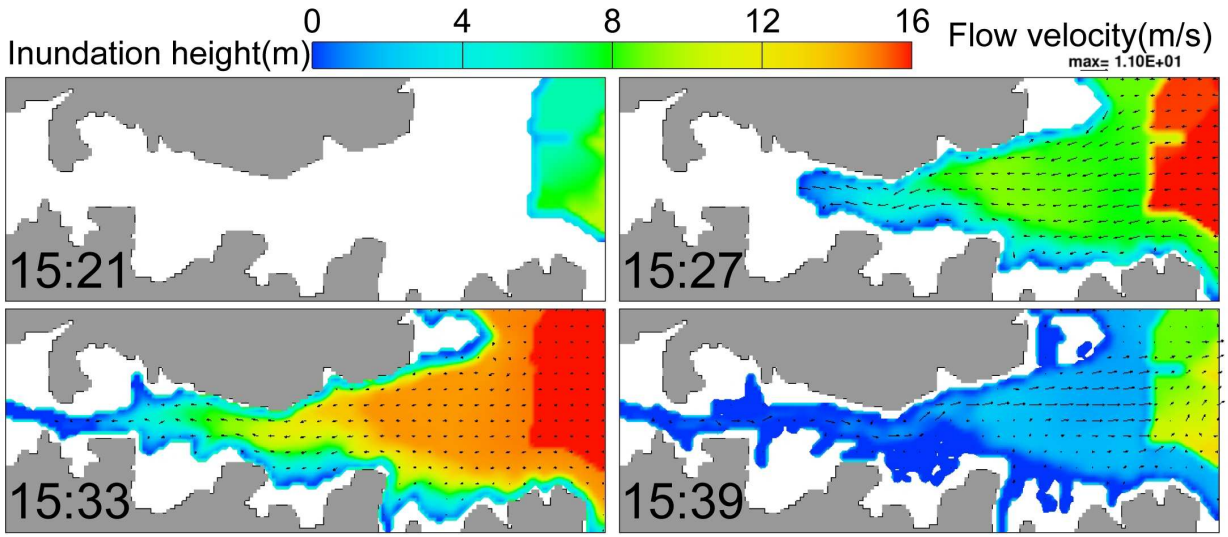

Figure 9. Distribution of inundation height and flow velocity

The buoyant force F_B acting on the buildings is calculated by the following formula;

$$F_B = \rho \times g \times (V - V_w) \quad (3)$$

where g is gravitational acceleration ($9.8 m/s^2$), V is the volume of the building to inundation height, and V_w is the volume of water entering the buildings.

The flow rate of the water entering the buildings was calculated by multiplying the area of the building openings below the inundation height on the seaward side A_s by the calculated flow velocity. The V_w value was limited by the height of the upper end of the highest opening on the seaward and landward sides and the inundation height in each floor of buildings. The value of V_w was also constrained by assuming the buildings were empty with an average pillar cross section of 500mm × 500mm and wall thickness of 200mm.

Evaluation of building damage

Figure 10 shows simplified free body diagrams for sliding, uplift, and overturning mechanisms. In the sliding model for pile foundations, the concrete in all of the piles is assumed to break when the tsunami load horizontal force is greater than 0.4 of the building weight. Therefore, we assumed that the resisting force of the pile foundation buildings in sliding was due to the shear strength of the rebar and the passive earth pressure, as shown in Figure 10. For spread foundation buildings in sliding we assumed that the resisting force was due to base friction and passive earth pressure. For pile foundations in uplift, we estimated the resisting force with and without pile resistance. For overturning, we calculated the overturning moment versus the resisting moment based on a center of rotation at the bottom edge of each building, as shown in Figure 10. In overturning of pile foundation buildings, we assumed that the resisting moment was composed of the pile skin friction and the weight of the building, and we assigned a larger skin friction force to the front piles than the back piles, whereas for spread foundation buildings, the resisting moment was only a function of the building weight.

Figures 11-13 show the estimated tsunami load (black line) and building resistance (red line) using these simplified models. Figure 13 shows that for buildings No.1 and No.2, the concrete in the piles break during the first tsunami run-up. Figures 11-13 show that building No.1 failed due to overturning during the tsunami run-up, building No.2 did not fail, and building No.3 failed due to sliding and overturning during the back wash. These results correspond with the observed building performance, where building No.1 failed landward, building No.3 failed seaward, and building No.2 did not fail.

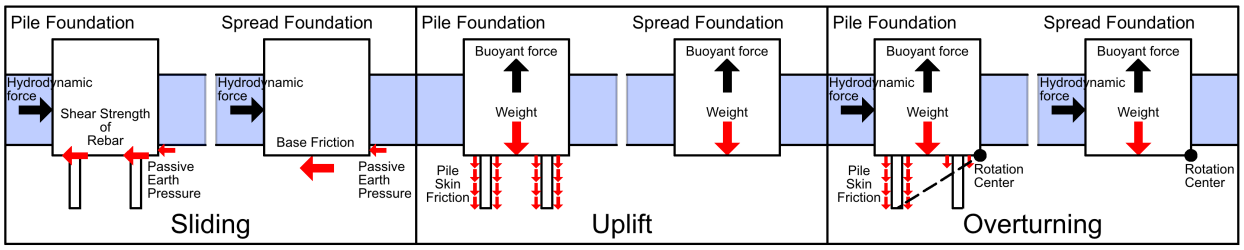

Figure 10. Evaluation model of sliding, uplift, and overturning

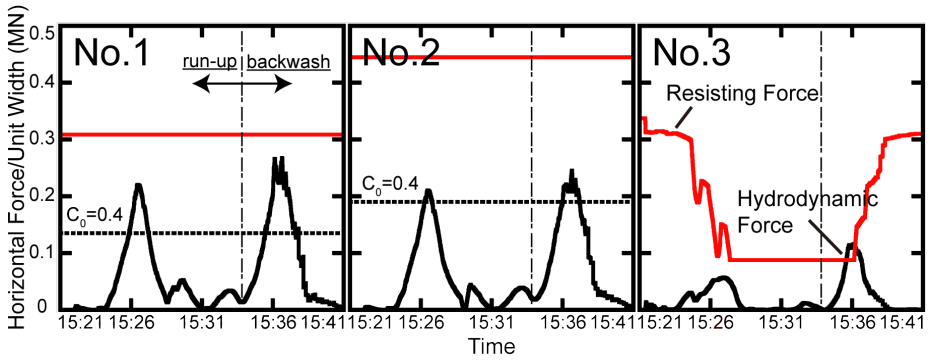

Figure 11. Hydrodynamic Force versus resisting force

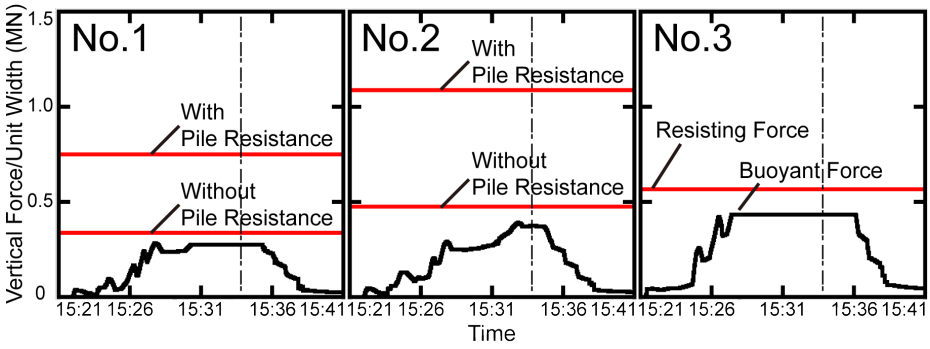

Figure 12. Buoyant force versus resisting force

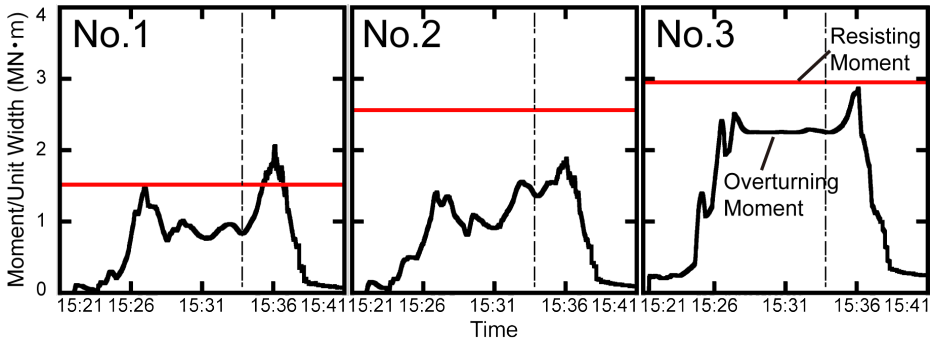

Figure 13. Overturning moment versus resisting moment

Conclusions

We conducted a 2D simulation of the tsunami run-up during the 2011 Great Tohoku Earthquake in the town of Onagawa to investigate the mechanisms and differences in overturning damage of three buildings. The simulation was based on video evidence of the first tsunami run-up. Based on the time histories of inundation height and flow velocity predicted by the 2D simulation, we estimated the hydrodynamic force and buoyant force acting on the buildings. The results of the analysis were able to qualitatively predict the differences in the type of building damage observed after the tsunami.

Acknowledgements

Several of the photographs used in the paper were taken by Professor Shuji Tamura, Tokyo Institute of Technology, and East Japan Earthquake Picture Project. Their permission for reuse of their photos is gratefully acknowledged. We would also like to thank Dr. Brian Carton for his help reviewing this article.

References

Koshimura, S. and Hayashi, S. (2012): Tsunami flow measurement using the video recorded during the 2011 Tohoku tsunami attack. *International Geoscience and Remote Sensing Symposium*, IEEE international, pp.6693-6696

Sugimura, Y. and Mitsuji, K. (2012): The survey of buildings overturned and carried out by tsunami. *Foundation Engineering and Equipment*, Vol. **40**, No.12, pp.71-75 (in Japanese).

Tokimatsu, K., Tamura, S., Suzuki, H. and Katsumata, K. (2012): Buildings damage associated with geotechnical problems in the 2011 Tohoku Pacific Earthquake. *Soil and Foundation*, Vol. **52**, No.5, pp.956-974

Nakano lab, Institute of Industrial Science, the University of Tokyo (2012): The survey report of building damage by earthquake and tsunami in the 2011 Great Tohoku Earthquake. (in Japanese)

http://sismo.iis.u-tokyo.ac.jp/Research.files/topic4.files/

Kiku, H. and Sugano, T. et al. (2012): Several in-site tests on liquefaction potential at peripheral ground of pile foundation pulled out by tsunami. *Proc. of 47th Japan National Conference on Geotechnical Engineering*, pp.1831-1832 (in Japanese).

Hirt, C.W. and Richardson, J.E. (1999): The modeling of shallow flows. *Flow Science, Inc., Technical Notes*, FSI-99-TN48R

Federal Emergency Management Agency (2008): Guideline for Design of Structures for Vertical Evacuation from Tsunamis. *FEMA P646*

Geospatial Information Authority of Japan (2011): Aerial photography (Fig.1),

Yahoo: East Japan Earthquake Picture Project (Fig.2a, 2b), http://archive.shinsai.yahoo.co.jp/, accessed 2015-02-28

Google: Google Street View (Fig.4a), https://www.miraikioku.com/, accessed 2015-02-28